The Cryosphere Discuss., doi:10.5194/tc-2016-282, 2017
Manuscript under review for journal The Cryosphere
Published: 3 January 2017

The Cryosphere Discussions
Open Access
EGU

Validation of satellite altimetry by kinematic GNSS in central East Antarctica

Ludwig Schröder[1], Andreas Richter[1], Denis V. Fedorov[2], Lutz Eberlein[1], Evgeny V. Brovkov[2], Sergey V. Popov[3], Christoph Knöfel[1], Martin Horwath[1], Reinhard Dietrich[1], Alexey Y. Matveev[2], Mirko Scheinert[1], and Valery V. Lukin[4]

[1]Technische Universität Dresden, Institut für Planetare Geodäsie, Dresden, Germany
[2]OAO Aerogeodeziya, St. Petersburg, Russia
[3]Polar Marine Geosurvey Expedition (PMGE), St. Petersburg, Russia
[4]Arctic and Antarctic Research Institute (AARI), St. Petersburg, Russia

Correspondence to: Ludwig Schröder (ludwig.schroeder@tu-dresden.de)

Abstract. Ice-surface elevation profiles of more than 30.000 km in total length are derived from kinematic GNSS observations on sledge convoy vehicles along traverses between Vostok station and the East Antarctic coast. The profiles have accuracies between 4 and 9 cm. They are used to validate elevation datasets from both radar and laser satellite altimetry as well as four digital elevation models. A crossover analysis with three different Envisat radar altimetry datasets yields a clear preference for the relocation method over the direct method of slope correction and for threshold retrackers over functional fit algorithms. The validation of Cryosat-2 low-resolution mode and SARIn mode datasets documents the progress made from baseline B to C elevation products. ICESat laser altimetry data are demonstrated to be accurate to a few decimeters over wide range of surface slopes. A crossover adjustment above subglacial Lake Vostok combining ICESat elevation data with our GNSS profiles yields a new set of ICESat laser campaign biases and provides new, independent evidence for the stability of the ice-surface elevation above the lake. The evaluation of digital elevation models reveals the importance of radar altimetry for the reduction of interpolation errors.

1 Introduction

Surface elevation data is crucial for a broad range of applications in polar sciences. Only satellite altimetry is able to provide this information with a high and nearly uniform accuracy and precision for almost the entire Antarctic ice sheets. This high accuracy also allows to infer temporal changes in ice surface elevation, which is of prime scientific interest in the context of ongoing climate change (Shepherd et al., 2012; Groh et al., 2014). However, systematic effects can deteriorate the derived elevation trend $\dot{h}$ and - if not corrected thoroughly - they might lead to misinterpretation of the observations (Arthern et al., 2001; Lacroix et al., 2009).

One crucial step in the processing of surface elevations from satellite radar altimetry (SRA) over ice sheets is the slope correction (Brenner et al., 1983). Due to the size of the beam-limited footprint of about 20 km in diameter the first reflection can originate from a location up to several kilometers away from the nadir in a sloping surface. Different approaches exist to

The Cryosphere Discuss., doi:10.5194/tc-2016-282, 2017
Manuscript under review for journal The Cryosphere
Published: 3 January 2017

correct this effect (e.g. Bamber, 1994; Roemer et al., 2007) but, as the corrections can exceed 100 m (Brenner et al., 2007), remaining model errors may introduce height errors of up to several meters. This is the major factor limiting the application of SRA in the steep and rugged coastal areas (Flament and Rémy, 2012).

Another issue when deriving ice-surface elevations from SRA data is the penetration of the electromagnetic signal into the upper firn layers. This results in a mixed return signal consisting of surface reflection and volume reflection (Ridley and Partington, 1988). Here, the selection of an appropriate retracking algorithm is essential. One approach to minimize the influence of the volume echo on the observed surface elevations is to retrack at the very beginning of the waveform (Davis, 1997). Another method is to apply appropriate corrections using parameters of the radar return waveform shape (Wingham et al., 1998; Flament and Rémy, 2012; Zwally et al., 2015).

For the Ice Cloud and Land Elevation Satellite (ICESat) mission these effects do not arise as the onboard altimeter uses laser signals. Hence, significantly higher accuracies can be achieved. Nonetheless, also those measurements are not free of systematic errors. Pointing errors and orbital variations (Luthcke et al., 2005) or saturation effects (Scambos and Shuman, 2016) may cause laser campaign biases which induce spurious trends of up to 2 cm/yr (Hofton et al., 2013; Gunter et al., 2014).

In order to quantify the impact of these errors and to evaluate methods for their correction, independent elevation data of high precision and accuracy is crucial. Here, we make use of ice-surface elevation profiles in central East Antarctica of more than 30.000 km of total length. These profiles are derived from kinematic GNSS (Global Navigation Satellite System, GPS and GLONASS in this case) observations carried out over more than one decade on sledge convoy vehicles along continental traverses. This set of surface-elevation profiles is made available for download on the data server PANGAEA (https://doi.org/10.1594/PANGAEA.869761).

2 Surface elevations from kinematic GNSS-profiles

2.1 Kinematic GNSS observations

The Russian research station Vostok is located in the central part of East Antarctica (106.8° E, 78.5° S). It is the main base for a wide range of scientific fieldwork related to the subglacial Lake Vostok. Between 2001 and 2015 several kinematic GNSS profiles have been measured in the area of the lake as well as on the scientific traverses from Vostok station to the East Antarctic coast.

Geodetic dual-frequency GNSS receivers with external antennas were used for the kinematic profiling as well as on the reference stations. Two different types of profiles can be distinguished with respect to the vehicles onto which the GNSS antennas were mounted. The first type are observations performed on lightweight snowmobiles. With the help of such profiles Richter et al. (2014) have shown that the surface elevation around Vostok station has been stable over the last decade confirming the results of permanent GNSS observations (Richter et al., 2008, 2014). The profiles acquired on snowmobiles provide accuracies of only a few centimeters and are thus well suited for precise studies on local elevation and elevation changes. However, due to logistic reasons they usually cover only a very limited area and are therefore not considered here.

The Cryosphere Discuss., doi:10.5194/tc-2016-282, 2017
Manuscript under review for journal The Cryosphere
Published: 3 January 2017

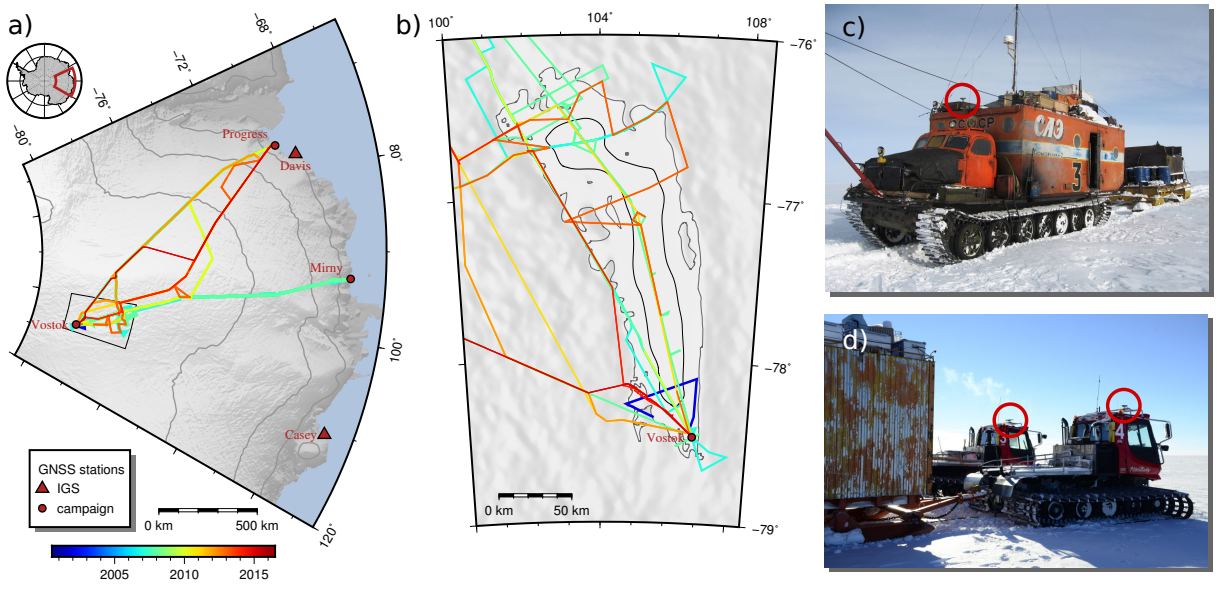

Figure 1. a) Overview of the kinematic GNSS profiles (color coded by their chronological sequence) and the GNSS reference stations used in the differential processing **b)** Detailed map of the profiles in the area of subglacial Lake Vostok (outline in gray, hydrostatic equilibrium area in black) **c)** Convoy vehicle of type STT-2 Kharkovchanka-2 (profile K10B) with antenna mounted on the container above the cabin (red circle) **d)** Convoy vehicles Kässbohrer PistenBully (profiles K14A and K14B) with antenna mounted on top of the cabins

The second type of observations are carried out on heavy convoy vehicles. Those are tractors on tracks, designed to pull sledges with containers for accommodation and fuel tanks (Fig. 1). Hence, they are ideal platforms for the measurement over very long distances. This is a precondition for the validation of satellite altimetry on a larger scale, as it helps to minimize the influence of regional peculiarities (Kohler et al., 2013). The disadvantage of such heavy platforms, compared to snowmobiles, is that they sink into the soft upper snow layers by up to several decimeters. The amount of the vehicle's subsidence, and thus of the height of the antenna above the snow surface, varies locally. Therefore, this antenna height has to be measured as often as possible along the traverse.

In the austral summer 2001/2002, our first surface elevation profile was acquired during a seismic convoy of the Russian Antarctic Expedition (RAE) along a 150 km transect in the southern part of Lake Vostok. During this traverse over 6 days a GNSS antenna was installed on the roof of a trailer, pulled by a traverse vehicle.

After this regionally limited campaign, much longer profiles were observed since 2006. In that time Mirny station (93.0° E, 66.6° S) was the coastal logistical hub for the supply of Vostok station by overland traverses. Several scientific observations were performed during these convoys (Masolov et al., 2001; Richter et al., 2013; Popov, 2015; Ekaykin et al., 2016). In the austral summer 2006/2007 kinematic GNSS profiles between Vostok and Mirny were observed on two convoy vehicles. For the first time these profiles cover all the distance of about 1.600 km from the remarkably flat ice surface above Lake Vostok down to the rugged terrain at the coast. In the following season these profiles were repeated on two vehicles.

The Cryosphere Discuss., doi:10.5194/tc-2016-282, 2017
Manuscript under review for journal The Cryosphere
Published: 3 January 2017

In 2009, Progress station (76.4° E, 69.4° S) became the main logistic hub for Vostok station. A first reconnaissance traverse from Progress to Vostok and back in 2007/2008 already included geodetic GNSS-equipment. Since austral summer 2009/2010, several profiles between these two stations were observed each season. A number of different routes were used according to the needs of further participating scientific groups, snow conditions or logistical constraints. Fig. 1 gives an overview of the locations and observation times of the routes as well as two impressions of the types of vehicles used. Table 1 contains detailed information about each individual profile.

2.2 GNSS data processing

We used the Bernese GNSS Software 5.2 (Dach et al., 2015) for the differential post-processing of the kinematic observation data. This processing yields a 3D coordinate of the GNSS antenna for each observational epoch in the terrestrial reference frame IGS08. Using those coordinates, a profile of ellipsoidal elevations referring to WGS-84 are derived. For most of the profiles multi-system GNSS receivers were used, i.e. observations from the Russian Global Navigation Satellite System (GLONASS) are logged in addition to the Global Positioning System (GPS). The increased amount of observation data improves the reliability of the solution significantly. As kinematic reference site in this differential positioning we utilised static observations from campaign sites, for example in Mirny or Progress, from an own permanent receiver in Vostok installed in early 2008 (for details see Richter et al., 2014) and additionally from the sites Casey and Davis of the IGS-network (see Fig. 1). To cope with the scarce sampling interval of the IGS-sites of 30 s, those static observations had to be interpolated to the rate of the kinematic receivers (mainly 5 s or 15 s, sf. Table 1). For that purpose we used WaSoft, a software tool developed by Wanninger (2000). We adopt the processing strategy of Fritsche et al. (2014), which corrects or parametrises the tropospheric and ionospheric delay, the antenna phase centre offsets and variations, solid earth tides and loading displacements. Special attention is paid to the resolution of the GNSS carrier phase ambiguities of the differenced observations. When the vehicle is halfway between Vostok and the coast, no baseline to a static reference station is shorter than 800 km. Then, only very robust ambiguity resolution strategies are able to produce satisfactory results. Therefore, in this case we used the Melbourne-Wübbena and the Quasi-Ionosphere-Free Linear Combination only. As this is the most critical step in processing, a thorough outlier screening of the fixed ambiguity solutions is essential. For this reason, we always used more than one, typically four to five, baselines to different reference sites. Undetected cycle slips lead to very large deviations of the affected baseline. Thus, by processing each baseline independently and comparing the results to the combined solution, the baseline causing large deviations can be identified and the undetected cycle slip has to be introduced manually.

2.3 Derivation of surface elevation profiles

The antenna trajectory resulting from the GNSS positioning has to be corrected for the height of the antenna above the local snow surface in order to derive surface elevation profiles. This vertical offset is not constant as the amount to which the vehicle sinks into the snow depends on the regionally varying surface snow properties, but also on the vehicle type (e.g. track width). For example, Kohler et al. (2013) had to employ additional laser measurements on another vehicle in order to retrieve the amount of vehicle subsidence because the antenna height was not measured repeatedly along their profiles. During our traverses

The Cryosphere Discuss., doi:10.5194/tc-2016-282, 2017
Manuscript under review for journal The Cryosphere
Published: 3 January 2017

we measured this antenna height offset AH several times each observation day for each profile. However, the representativity of a single offset measurement may still be limited due to small-scale surface structures (sastrugi) at the locations of the measurements. Thus, to obtain a specific offset for each single epoch i, we use a regional average

$$AH_i = \frac{\sum_j (d_{ij}^{-1} \cdot AH_j)}{\sum_j d_{ij}^{-1}}, \quad (1)$$

where d_{ij}^{-1} is the inverse distance between the position at epoch i and the position of the antenna height measurement AH_j.

Furthermore, a permanent tilt of the moving vehicles had to be considered. While driving in soft snow, especially when pulling heavy sledges, the nose of the vehicle gets lifted up while the rear buries deeper. This dynamic effect is not determined directly as our offset measurements are taken during stops when the vehicle stands upright. However, an instantaneous jump in antenna elevation from GNSS positioning is observed whenever the vehicle stops. Depending on the antenna's position on the vehicle, it can reach 20 cm. These jumps are used to correct the measurement AH for the vehicle dynamics. For this purpose we interpolate the *elevations in movement* (i.e. velocity > 1 km/h) to the position of the antenna height measurement by fitting a quadratic function within a distance of 100 m around this point and comparing it to the average *elevation in rest*.

To reduce the noise and to make the along-track resolution more comparable to the altimetric elevations we applied a low-pass filter to the original antenna trajectory. The typical along-track spacing of the radar altimeter data is several hundreds of meters. Furthermore, due to the diameter of the pulse limited footprint of about 2 km the measurement represents an average elevation of this area. In contrast, the GNSS profiles sample the elevation along their track with a very dense spacing. Depending on the sampling interval (Table 1) and the velocity of the vehicles (about 7 km/h) the usual point distance is in the range of 10 to 30 m. We applied a Gaussian filter with a Gaussian sigma of 60 m and a total length of 180 m. This reduces not only the measurement noise, but also variations due to vehicle dynamics or very small-scale topography (e.g. sastrugi). In addition, the trajectory positions are thinned out to an equidistant interval of 30 m. This reduces substantially the data amount without loss of information (e.g. data logged during overnight stops of the convoy).

A comparison between kinematic GNSS profiles and satellite altimetry products requires a correction due to the different treatment of the permanent tide in the reference systems underlying both techniques. According to McCarthy and Petit (2004) the International Terrestrial Reference Frame (ITRF) is a "conventional tide free" frame. Hence, all tidal effects including the permanent effect have been removed from the coordinates of the reference stations. Our elevation profiles are consequently also conventional tide free. Altimetric elevations, in contrast, refer to the "mean tide" system. The GNSS elevations are converted to this mean tide system using Eq. 7.14a of Petit and Luzum (2010), which is a function of the latitude and amounts to about -10 cm at 70°S.

2.4 Accuracy estimates

Accuracy estimates for the epochwise coordinates consist of estimates of the quality of the antenna positioning and an additional uncertainty due to the reduction to the snow surface. In a first step we assess the quality of the GNSS processing. The formal coordinate accuracies reported by the processing software are too optimistic as they do not account for non-white noise components. A more realistic measure is found by comparing multiple baseline solutions. As mentioned in Sect. 2.2, the ambi-

The Cryosphere Discuss., doi:10.5194/tc-2016-282, 2017
Manuscript under review for journal The Cryosphere
Published: 3 January 2017

Table 1. Overview of the kinematic GNSS-profiles. Accuracy estimates are the mean elevation error from GNSS processing (from differences between combined and single baseline solutions) $\overline{RMS_{BL}}$, the mean formal accuracy of snow surface elevation $\overline{RMS_S}$ and the empirical mean crossover difference between profiles of one season $\overline{RMS_X}$.

Profile	Vehicle (Type)	Area*	Duration	Length [km]	Sampling [s]	$\overline{RMS_{BL}}$ [cm]	$\overline{RMS_S}$ [cm]	$\overline{RMS_X}$ [cm]
K01A	trailer (tracks)	V	2001-12-07 - 2001-12-12	150	30	5.0	5.0	-
K07A	tractor (Ishimbai)	V→ M	2007-01-07 - 2007-03-05	2280	5	3.8	4.0	8.0
K07B	tractor (Ishimbai)	V→ M	2007-01-09 - 2007-01-23	580	5	2.9	4.3	6.4
K07C	tractor (STT-1)	V→ M	2007-02-04 - 2007-03-05	1270	5	3.3	3.9	8.6
K08A	tractor (Ishimbai)	V→ M	2008-01-11 - 2008-02-18	1720	5	2.3	2.5	8.4
K08B	tractor (ATT)	M	2008-02-19 - 2008-03-13	400	5	1.9	3.3	6.5
K08C	trailer (sledge)	P→ V→ P	2008-01-06 - 2008-02-07	2890	5	1.5	1.7	-
K08D	tractor (STT-2)	V→ M	2008-02-08 - 2008-03-14	1960	5	2.4	2.8	6.7
K10A	tractor (ATT)	V→ P	2010-01-24 - 2010-03-18	1690	15	1.6	2.2	6.1
K10B	tractor (STT-2)	V→ P	2010-01-31 - 2010-03-15	1460	15	2.2	2.5	6.1
K11A	tractor (Kässbohrer)	P→ V→ P	2011-01-07 - 2011-02-08	1690	15	1.7	2.3	4.3
K11B	tractor (Kässbohrer)	P	2011-02-13 - 2011-02-14	80	15	1.5	2.9	4.3
K12A	tractor (Kässbohrer)	V→ P	2012-01-25 - 2012-02-11	1560	5	2.8	2.9	8.4
K12B	tractor (Kässbohrer)	V→ P	2012-01-25 - 2012-02-11	1560	5	2.2	2.4	8.4
K13A	trailer (sledge)	V→ P	2013-01-20 - 2013-02-12	2140	5	2.4	2.6	6.2
K13B	tractor (Kässbohrer)	V→ P	2013-01-20 - 2013-02-15	2220	5	2.2	2.3	6.2
K14A	tractor (Kässbohrer)	V→ P	2014-01-22 - 2014-02-11	1480	5	2.6	3.1	7.1
K14B	tractor (Kässbohrer)	V→ P	2014-01-22 - 2014-02-11	1550	5	3.2	3.4	7.1
K15A	tractor (Kässbohrer)	V→ P	2015-01-21 - 2015-02-03	1560	15	1.5	2.0	8.1
K15B	tractor (Kässbohrer)	V→ P	2015-01-21 - 2015-02-03	1580	15	2.1	2.5	8.1

* V..Vostok, M..Mirny, P..Progress

guity resolution is a critical step in the GNSS data processing. Unrecognized cycle slips can distort profile sections over several kilometers and are thus not removed by the low-pass filter. However, such instances are identified within independent solutions using different reference sites. The average baseline coordinate differences RMS_{BL} are used to derive realistic estimates for the accuracy of the kinematic positioning. Mean baseline differences in the vertical component are shown for each profile in column $\overline{RMS_{BL}}$ of Table 1 and are in general on the order of 3 cm.

An additional source of uncertainty is imposed by the reduction of the GNSS antenna elevation to the snow surface. This reduction varies regionally due to varying snow surface characteristics. Thus, besides the error of the offset measurements themselves, the offset corrections, obtained by Eq. (1), contain an additional interpolation error. We assess both types of errors using semivariograms. Here, fit a linear function to the squared differences between the measurements of the antenna height

The Cryosphere Discuss., doi:10.5194/tc-2016-282, 2017
Manuscript under review for journal The Cryosphere
Published: 3 January 2017

offsets, with respect to the distances between those measurements. We obtain a constant part of 6 cm, which relates to the uncertainty of the antenna height measurement itself. It is potentially affected by local surface features (sastrugi) and residuals in the dynamic tilt correction. The distance related additional uncertainty is 0.25 cm/km and accounts for the specific distance between the location of the respective offset measurement and the location to be interpolated. Using these values, the accuracy of the antenna height reduction through inverse distance interpolation (RMS_{AH}) is derived. Hence, the total accuracy measure for a single surface elevation observation is obtained by

$$RMS_S = \sqrt{{RMS_{BL}}^2 + {RMS_{AH}}^2}. \quad (2)$$

A rigorous empirical test for the total accuracy estimate is performed by the calculation of height differences at crossover locations of two different profiles of the same season. The time elapsed between the two passes over this location is typically between a few minutes and some days, thus the surface elevation is assumed unchanged. As the differences Δh are calculated from two passes, the accuracy RMS_X of a single profile at the crossover location is given by

$$RMS_X = \Delta h / \sqrt{2}. \quad (3)$$

For our profiles we obtain RMS_X in the range of 4 to 9 cm (see Table 1). This is slightly higher than the RMS_S because it includes also the effect of vehicle dynamics. Nevertheless, it is a conservative estimate as in these crossovers the elevations of the second profile are affected by the disturbances of the snow surface originating from the first vehicle pass.

2.5 Elevation changes

Our kinematic GNSS profiles do not always coincide in their acquisition time with the satellite altimetry data to be validated. Therefore, when comparing the GNSS-derived elevations with altimetry products, it is crucial to know to what extent elevation changes occurred between their respective observation epochs. While crossover differences within one expedition are used for accuracy estimates, the elevation differences in crossovers between profiles of different years allow to assess temporal rates of surface elevation changes ($\dot{h}$). Figure 2a shows that the obtained surface elevation rates are very small over the whole area. In Fig. 2a they are averaged at 20 km-blocks to reduce random noise. However, the rates shown may still be affected by systematic errors effective over longer distances. One potential error source, in addition to those mentioned in Sect. 2.4, is the impact of human activities on the snow surface. The immediate vicinity of the stations is obviously heavily affected but this is not the only region which had to be handled with care. For five decades the convoy between Mirny and Vostok used the same route. Especially above 3000 m, the heavy convoy vehicles and cargo sledges had followed exactly the same track in order to cope with the soft snow. This resulted in enhanced snow compaction along the track and the accumulation of a continuous ridge of several decimeters in height which is even visible on satellite imagery. The elevations and elevation changes along this part of the traverse are not representative for this area and are thus excluded from all subsequent studies. The profiles acquired on the modern Kässbohrer tractors are not prone to this effect since their wider tracks and relatively small weight relieves these vehicles from the need to reuse a pre-existing track.

The largest rates, but also the largest variations, are found on the traverse to Mirny. In the lower parts this is not an effect of anthropogenic disturbance. As the snow is much harder there, the tractors do not repeat the exact tracks of their predecessors.

The Cryosphere Discuss., doi:10.5194/tc-2016-282, 2017
Manuscript under review for journal The Cryosphere
Published: 3 January 2017

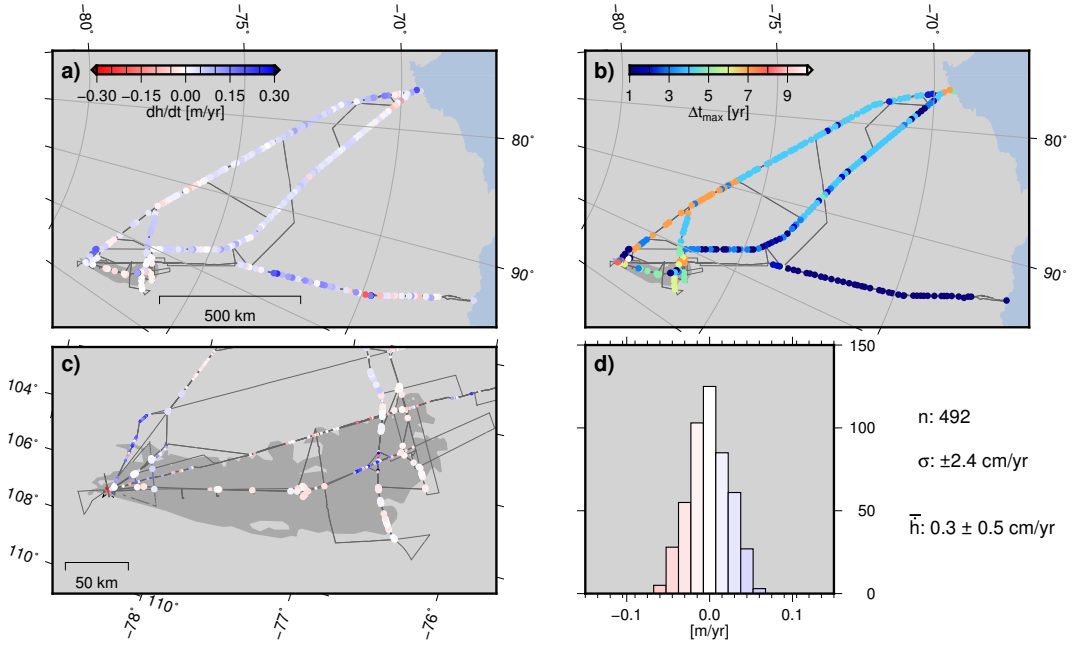

Figure 2. a) Elevation change rate from crossovers between different seasons (20 km block mean values). **b)** Maximum observation time span of crossover differences within each block. **c)** $\dot{h}$ in the Lake Vostok region. Crossovers on the convoy track or with $dt < 5$ yr are plotted half sized. **d)** Distribution of the valid (full sized) crossovers from c in the Lake Vostok region.

Nevertheless, the rates obtained in this area rely on only one year time span between the measurement of those profiles and must therefore be treated with care. In the areas where the time span is longer, very small rates are obtained. Averaging all 18,000 $\dot{h}$ by introducing weights according to the time span results in a mean elevation change over the entire area of 4 cm/yr and a standard deviation (σ) of a single crossover rate of ±11 cm/yr.

A detailed look into the results in the Lake Vostok region is given in Fig. 2c and d. In order to avoid the limitations arising from short observation time spans, we used only crossovers spanning five years or more. The weighted mean $\bar{\dot{h}}$ of the 492 crossover differences in this area is 0.3 cm/yr with a standard deviation of a single rate of ±2.4 cm/yr. The $\dot{h}$ values are not uncorrelated, especially due to possible systematic biases (e.g. antenna height reduction) which affect multiple crossovers of a profile. Therefore, for the accuracy of the mean $\bar{\dot{h}}$ we only consider the number of combinations of independent profiles (27) in the estimation, resulting in a standard error of ±0.5 cm/yr. This comprises both, real variations in surface-elevation change rate and observation uncertainties. These results agree very well with the elevation changes observed by measurements on snowmobiles around Vostok station (Richter et al., 2014, 0.1 ±0.5 cm/yr). The latter profiles have a higher accuracy but yield a smaller amount of crossovers affected by higher spatial correlation.

We conclude that the elevation change rates are very small in the region under investigation, but their spatial pattern is not determined with homogeneous reliability due to the short observation time span in some areas. Our profiles shall be used nevertheless for the validation of SRA, which is subject to much larger uncertainties, especially in coastal regions. Thus we

The Cryosphere Discuss., doi:10.5194/tc-2016-282, 2017
Manuscript under review for journal The Cryosphere
Published: 3 January 2017

consider the surface elevation over the entire region as stable and do not correct for elevation changes. This choice will be justified further in Sect. 3.3.3.

3 Validation of satellite altimetry

3.1 Data

3.1.1 Envisat

We validate different altimeter missions to reveal characteristic effects of the respective techniques and approaches to derive optimum results. Conventional altimeter systems usually use signals in Ku-band and have a beam limited footprint of 10 to 20 km. Over ice sheets their signals penetrate into the upper firn layer, resulting in a return signal containing surface as well as volume scattering fractions. As an example for a conventional pulse limited radar we validate the Envisat mission, operated by the European Space Agency (ESA). We use the Ku-band measurements of its altimeter system RA-2 acquired during the entire operation period (May 2002 to April 2012). In the Level 2 product (SGDR V2.1) the slope induced error is corrected using the relocation method (Bamber, 1994). This algorithm is designed to locate the measurement to the position where the first return signal comes from. The ESA dataset contains results from two types of return waveform retrackers applicable over ice sheets, ICE1 (based on the Offset Centre Of Gravity (OCOG) retracker by Wingham et al., 1986) and ICE2 (a functional fit developed by Legrésy et al., 2005). We use both retrackers to compare their performance.

The Goddard Space Flight Center (GSFC) developed an own processing chain for radar altimetry with slightly different approaches for some steps in deriving the surface elevations. Here, the direct method of slope correction is applied, which corrects the measurement in the nadir. This reprocessed Level 2 dataset is called Ice Data Record (IDR) and contains also different retrackers. We use the GSFC V4 β-retracker as Brenner et al. (2007) summarise that this algorithm provides more accurate absolute elevations than threshold based methods.

To remove potentially corrupted observations from the data, we used the *measurement confidence flag* (which is identical in ESA's SGDR and GSFCs IDR datasets) to find recorded distances out of range and to identify problems of the onboard processing and data handling, of the ultra stable oscillator, of the automatic gain control (AGC) or of the waveform samples. In addition to these instrumental errors we removed shots where the GSFC retracking algorithm failed as indicated by the *retracking problem flag*. In the SGDR data we furthermore used the overall *fault identifier* and the flag indicating that the ICE1 retracking in Ku-band was not successful.

3.1.2 CryoSat-2

Compared to the conventional SRA, ESA's CryoSat-2 has an improved resolution and accuracy due to its innovative design. In the smooth interior of the ice sheets the altimeter operates in the Low Resolution Mode (LRM) which is a conventional pulse limited observation mode as in the missions before. Above steeper terrain, the altimeter is switched to SARIn Mode. In this mode, the Synthetic Aperture Radar (SAR) processing considerably improves the along track resolution utilizing the

The Cryosphere Discuss., doi:10.5194/tc-2016-282, 2017
Manuscript under review for journal The Cryosphere
Published: 3 January 2017

Doppler/delay shift. Hence, the beam limited footprint is subdivided in flight direction into stripes of only 250 m length. The interferometric processing of the reception times at the two antennas allows the determination of the across track direction of the point of closest approach (Wingham et al., 2006a).

We compare two different processing versions, Baseline B and C, of ESA's L2I dataset. The "I" in the product identifier stands for the In-depth dataset. It provides more parameters and flags and, over land, offers an additional feature relevant for our study. In the basic L2 product the *SARIn ambiguity flag* indicates an elevation difference between altimetry and a DEM exceeding 50 m. In this case the interferometric angle is considered as erroneous and the measurement position is set to nadir. In the L2I product, however, this is not applied. This product allows us, therefore, to validate the data also at the margins where the a priori DEM itself is prone to large uncertainties (see Sect. 4). As an alternative approach to identify outliers in the interferometric angle, we used the coherence flag and additionally excluded all measurements with a cross-track direction exceeding 1° (corresponding to the very edge of the antenna beam). Furthermore, we exclude all data where the respective *retracker height error flag* indicates problems in the determination of the retracking point. For Baseline B, the waveform is processed using the CFI retracker (Wingham et al., 2006a). In Baseline C two additional retrackers have been applied on the LRM data: A threshold based OCOG-retracker and another functional fit retracker called UCL, which is based on the Brown-model.

3.1.3 ICESat

In contrast to radar altimeters, the laser signal of the ICESat mission has a footprint of only 65m and does not penetrate into the snow pack. Hence, surface-elevation accuracies at the decimeter level can be achieved (Schutz et al., 2005) which are almost comparable to our kinematic GNSS profiles. We use GLA12 elevation data from Release 34 (R34).We apply the saturation correction to the elevations and exclude all data where flags indicate off-nadir operation, orbit maneuvers or any other degraded orbit accuracy. We also remove data where the attitude flag indicates any problem with star trackers, gyro or the laser reference sensor. In order to exclude data affected by forward scattering in clouds or drifting snow (e.g. Siegfried et al., 2011), we reject all returns with a gain value exceeding 200, with a reflectivity below 10%, with a misfit between received waveform and a Gaussian model exceeding 0.03 V or for which more than one waveform is detected (Bamber et al., 2009).

3.2 Methods

3.2.1 Crossover comparison

Our validation approach is the following: We assess how accurately the altimetry data reflects the actual surface elevation at the nominal positions of the altimetry data.

Our approach of referring the altimetry data to pointwise positions is a pragmatic choice. As a matter of fact, altimetry observes some average elevation over an extended footprint area. The footprint size amounts to tens of meters for ICESat, a few hundreds of meters for CryoSat-2 in SARIN mode, and a few kilometers for ENVISAT and CryoSat-2 in LRM mode. The LRM mode footprints additionally depend on surface roughness and on the applied retracker. The average altimeter footprint

The Cryosphere Discuss., doi:10.5194/tc-2016-282, 2017
Manuscript under review for journal The Cryosphere
Published: 3 January 2017

elevations will generally differ from the elevation at the nominal altimetry data position. For rugged terrain this discrepancy will be larger than for smooth terrain. Here we comprise this discrepancy under the altimetry error.

An alternative approach (not followed here) would be to observe, by kinematic GNSS, two-dimensional grids of the topography of the altimeter footprints. Then we could calculate a GNSS-based average footprint elevation and compare it to the altimetry data. This approach faces the theoretical problem of exactly defining what the altimeter footprint is. In other words, if we refrain from regarding altimetry as a pointwise measurement, we face the problem of exactly defining what altimetry ought to measure instead. The definition would need to be complicated. The alternative approach moreover faces the practical problem that the required two-dimensional observations are just not available along the 30,000 km of kinematic GNSS profiles.

We validate the surface elevation data derived from satellite altimetry by applying the crossover method, outlined in Sect. 2.4, to the intersections of the along-track altimetric profiles with our kinematic GNSS profiles. The along-track data point spacing amounts to 172 m for ICESat (Schutz et al., 2005), 250 m for CryoSat-2 (Wingham et al., 2006a) and 400 m for Envisat (ESA, 2007). Thus, in all cases the sampling interval exceeds by far that of the GNSS profiles. Because of the spatial averaging over the footprint area, the altimetry data represents smoothed profiles. The smoothing of the GNSS profiles (Sect. 2.3) allows thus for consistency in our comparison.

The largest error source for radar altimetry over a distinctive topography results from the slope correction. Brenner et al. (2007) found that crossover differences between ICESat and Envisat are less than 3 m for slopes below 0.1°, but up to 50 m and more for slopes above 0.7°. Hence, the validation of SRA needs to consider different surface slopes. Brenner et al. (2007) or Helm et al. (2014) binned their elevation differences with ICESat with respect to the slope. The obtained quasi-continuous functions clearly depict the growing differences with increasing surface slope. The amount and spatial coverage of our crossovers does not allow a comparison in such a high sampling of slope. Instead, we investigate regions of different characteristic slope in separate histograms. This allows us not only to calculate a mean and standard deviation for each zone but also to identify deviations from a Gaussian distribution. Those histograms display the full range of results including potential outliers. In order to reduce their impact, however, an iterative 5-σ filter is applied in the calculation of the mean and standard deviation.

We subdivide the region under investigation into four zones according to their mean surface slopes: >0.5°, 0.5 - 0.15°, <0.15° and, as a subset of the latter characterized by extremely little surface roughness, the hydrostatic equilibrium area of subglacial Lake Vostok. The crossovers differences between Envisat data and the GNSS profiles (Fig. 3) clearly demonstrate the relationship between slope and SRA errors and motivates our subdivision. The first zone comprises the coastal areas. Outliers and large errors in the SRA elevations are frequent there due to the rugged topography. On the other hand, in this zone typically the largest elevation changes can be expected. Hence, this zone introduces the largest uncertainties in ice-mass balance estimates based on SRA (Wingham et al., 2006b). The subsequent zone of intermediate slopes is still close to the coast and of low elevations. It may therefore also be subject to significant elevation changes. At the same time, SRA provides a better accuracy there compared to the first zone. The third zone comprises the flat interior of the ice sheet. Elevation changes are generally small here but, because of its vast areal extent, nevertheless important for mass balance studies. The ice above Lake Vostok, constituting our fourth zone, floats in hydrostatic equilibrium (Ewert et al., 2012). Surface gradients are very

The Cryosphere Discuss., doi:10.5194/tc-2016-282, 2017
Manuscript under review for journal The Cryosphere
Published: 3 January 2017

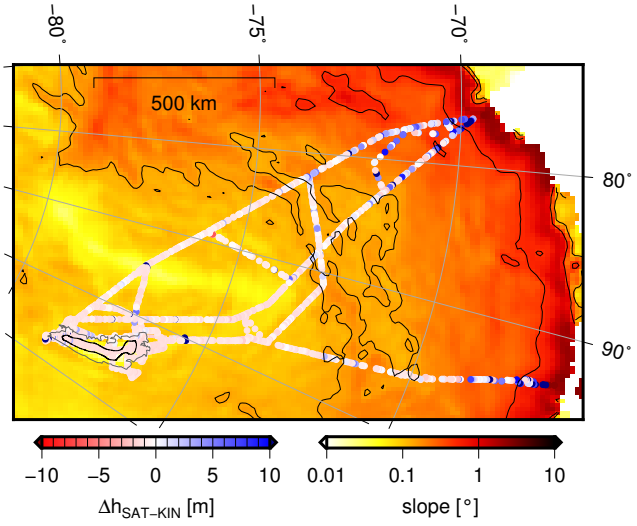

Figure 3. Crossover differences between Envisat (ESA, relocated, ICE1 retracker) and the kinematic GNSS profiles. The black contour lines mark the borders between the different zones of slope (0.15° and 0.5°) and the hydrostatic equilibrium area of Lake Vostok (outline in gray from Popov and Chernoglazov (2011)).

small and homogeneous in this area. Thus, the influence of the slope induced error vanishes, offering a unique opportunity to study other effects.

3.2.2 ICESat campaign biases

Due to the smaller footprint size, the ICESat surface elevations are less sensitive to surface slope than SRA. However, the GLAS altimeter was operated in several laser operation campaigns. Between the campaigns systematic biases exist. If not corrected carefully, these biases corrupt the inference of temporal surface-elevation changes and estimates of $\dot{h}$. To determine those biases, different surfaces have been used, including the salt flat Salar de Uyuni (Fricker et al., 2005), the global oceans (Urban in Scambos and Shuman, 2016; Gunter et al., 2009), the ice surface above Lake Vostok (Ewert et al., 2012), the Antarctic low precipitation zone (Hofton et al., 2013; Gunter et al., 2014) or leads and polynyas in sea ice areas (Zwally et al., 2015). The estimated biases differ significantly between different data releases and, within the same release, depending on the surface used for calibration.

Within the shoreline of subglacial Lake Vostok (Fig. 1b, 100–108.5 °E, 76–79 °S) Ewert et al. (2012) applied a least squares adjustment of crossover differences between ascending and descending ICESat (I) elevation profiles, acquired during laser campaigns i and j (Δh_{ij}^{I-I}). To cope with the lack of an absolute reference, these authors introduced a zero-sum condition. As a consequence, the laser campaign biases were determined as relative biases, relating to their overall average. This method relies essentially on the assumption of a stable surface throughout the ICESat observation period. This assumption is justified by the observational results of Richter et al. (2008).

The Cryosphere Discuss., doi:10.5194/tc-2016-282, 2017
Manuscript under review for journal The Cryosphere
Published: 3 January 2017

Using the ice-surface above Lake Vostok we derive a new set of laser campaign biases for release 34. In addition to the ICESat crossovers (I) used by Ewert et al. (2012) we now also include crossover differences between ICESat and our kinematic GNSS profiles (Δh_{iq}^{I-K}) and crossover differences between different GNSS profiles (Δh_{pq}^{K-K}). Including the unbiased GNSS profiles allows us to solve for the surface-elevation change rate $\dot{h}$ between the respective observation epochs t as an additional parameter and thus to overcome the assumption of a stable surface. Instead, we are hence able to separate real elevation trends from the apparent trend implied by the laser campaign biases b. Furthermore, the incorporation of the unbiased GNSS elevation profiles allows to avoid the zero-sum condition and thus to determine absolute laser campaign biases. Combining all crossover differences results in three different types of observation equations:

$$\begin{aligned} \Delta h_{ij}^{I-I} &= b_i - b_j + \dot{h}\Delta t_{ij} + \epsilon \\ \Delta h_{iq}^{I-K} &= b_i + \dot{h}\Delta t_{iq} + \epsilon \\ \Delta h_{pq}^{K-K} &= + \dot{h}\Delta t_{pq} + \epsilon \end{aligned} \tag{4}$$

To account for the individual accuracy of each GNSS profile, we introduce the epoch-wise elevation uncertainty RMS_S as weights for the elevations. As shown in Sect. 2.4 the empirical intra-expedition crossover differences RMS_X are about 5 cm larger. For this reason we add 5 cm to each RMS_S. For the ICESat elevations, in contrast, we assume a homogeneous standard deviation of 10 cm.

3.3 Results

3.3.1 Envisat

The validation of the Envisat data (Fig. 4) shows that in the flat interior all processing versions provide precise elevations. Nevertheless, the crossovers over Lake Vostok reveal significant differences between the three retracker versions. With 51 and 44 cm the standard deviations of the two functional fit retrackers (ICE2 and β-retracker) yield similar results, while the precision of the ICE1-retracked data with only 22 cm is better by a factor of two. This confirms the findings of Davis (1997) of a superior precision of threshold retrackers. With respect to the kinematic GNSS profiles, the mean bias of all processing versions is negative. This can be explained by the penetration of the radar signal into the upper firn layers. However, significant differences between the retrackers are evident here too. Compared to the ICE1-retracker, the mean reference surface of the ICE2 functional fit is 90 cm lower. Thus the influence of variations in firn pack properties is much stronger on this retracker. Between different datasets, a comparison of the biases of different retrackers should be treated with care. Here, elevation differences might also be caused by other sources as a different instrumental calibration value or alternative models for range correction.

Compared to Lake Vostok where the slope effect is negligible, significant differences can already be observed in the zone of least slopes (<0.15°). Even the smooth topography there introduces additional uncertainties of about 30 cm for the relocated ESA data and 1.5 m for the GSFC data corrected by the direct method. Furthermore, the mean biases are shifted in the positive direction. The histograms reveal that this is a consequence of a deviation from the Gaussian distribution of the crossovers. The increased amount of positive differences means that the GNSS-elevation is lower than the altimeter value. This is a

The Cryosphere Discuss., doi:10.5194/tc-2016-282, 2017
Manuscript under review for journal The Cryosphere
Published: 3 January 2017

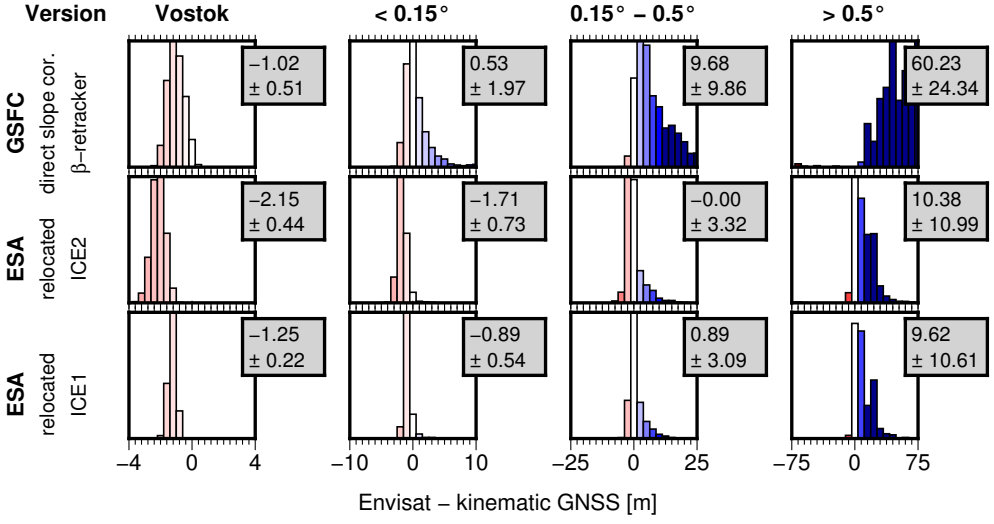

Figure 4. Histograms, means and standard deviations of crossover differences between different Envisat datasets and kinematic GNSS profiles for four zones of characteristic surface slope. The range of the histograms is adjusted according to the values found in each zone, the color scale is the same for all histograms. The displayed crossover differences contain uncertainties in the kinematic GNSS profiles (4 - 9 cm) and possible elevation changes between the observation epochs of both techniques in addition to the uncertainty in the Envisat data.

consequence of the inability of the radar signal to observe depressions which are significantly smaller than the beam-limited footprint diameter (Brenner et al., 2007). For all versions, this effect increases progressively as the slope and hence also the magnitudes of the depressions gets bigger. In the intermediate slope zone the standard deviations of the ESA datasets grow to 3 m and in the coastal zone up to 10 m. Here, the differences between the two ESA retrackers become negligible. For the GSFC product those errors are even significantly larger. Thus, our results support a clear preference for the relocation method. Nevertheless, in zones of larger slopes the error of the slope correction becomes the dominating uncertainty contribution.

To avoid loss of tracking, Envisat switched the tracking bandwidth from high resolution to two lower resolution modes when approaching steeper terrain. We analysed the performance of modes separately. Table 2 shows the results of each mode in the different zones. The number of crossovers indicates that the majority of data, even close to the coasts, was acquired in high resolution mode. In the central zone the accuracy of the lower resolution data is, as expected, worse. In the coastal zone, however, the other modes yield better results (if their small number of crossovers is considered as representative). The variations of the mean biases demonstrates in turn, that these mode switches induce offsets in the data. We agree therefore with Brenner et al. (2007) not to use the sparse data of the lower resolution modes for precise elevation change studies.

3.3.2 CryoSat-2

The results of the validation of CryoSat-2 are shown in Fig. 5. A comparison with those from Envisat (Fig. 4) clearly shows the advantage of the SARIn mode in zones of larger slopes. Furthermore, a comparison of the recent Baseline C version with the previous Baseline B documents the improvements made by solving several issues.

The Cryosphere Discuss., doi:10.5194/tc-2016-282, 2017
Manuscript under review for journal The Cryosphere
Published: 3 January 2017

Table 2. Statistics of crossover differences between different Envisat resolution modes with kinematic GNSS profiles similar to Fig. 4. Outliers ($> 5\sigma_{\Delta h}$) are excluded iteratively. Each set of statistics contains $\overline{\Delta h} \pm \sigma_{\Delta h}$ and the number of valid crossovers (sums can differ from the total number due to outlier rejection).

Dataset	Vostok		< 0.15°		0.15° - 0.5°		> 0.5°	
	[m]	#	[m]	#	[m]	#	[m]	#
total (ESA, ICE1)	-1.25 ±0.22	10081	-0.89 ±0.54	120888	0.89 ±3.09	32524	9.62 ±10.61	3736
high res. (320MHz)	-1.25 ±0.22	10078	-0.89 ±0.54	120717	0.89 ±3.09	32470	9.89 ±10.62	3634
medium res. (80MHz)	-0.86 ±0.22	3	-0.62 ±1.01	136	1.29 ±3.33	48	-0.15 ±1.67	96
low res. (20MHz)	2.20 ±0.12	2	0.01 ±1.26	39	-0.10 ±1.60	6	2.94 ±5.72	6

A primary issue solved from Baseline B to C was a range bias of 67 cm in SARIn and 20 cm in LRM data (Scagliola and Fornari, 2015). In the SARIn data this bias reduction is clearly visible in all zones. Besides that, no major changes are evident and also the standard deviations remain the same. Comparing the Baseline B LRM with the respective CFI-retracked version of Baseline C, we find a significant improvement in standard deviation. The refinements in the retracking procedure itself, described by Bouffard (2015), are probably responsible for those improvements. This holds especially true in the zones of stronger slopes where the retracking is more challenging. In the practically absence of slope related effects on Lake Vostok, the correction of the range bias is also evident in the LRM data.

The main improvement in performance of the Baseline C LRM data, however, has been introduced by adding two additional retrackers (UCL and OCOG). The OCOG retracker reaches standard deviations of about 20 cm over Lake Vostok, which is similar to the corresponding ICE1 retracker for Envisat. In contrast, the functional fit models show standard deviations of ~50 cm which is similar to the results of the ICE2 retracker of Envisat. For the entire low slope zone (<0.15°) we obtain similar results when comparing CryoSat LRM to Envisat. In the intermediate zone (0.15°-0.5°) the two missions cannot be compared directly as the statistics for CryoSat only relate to the sub-zone where the LRM is applied, which covers only the gently sloping areas. It should be noted that even though SARIn mode is usually applied in coastal regions only, there is still some SARIn data available over Lake Vostok. On July 28th 2010 and the first week of June 2013 CryoSat-2 observed whole profiles across Antarctica in SARIn mode and passed also our region under investigation (including Lake Vostok) several times. These profiles allow us to directly compare the different modes and in the case of Lake Vostok the performance of their retrackers. The first column of Fig. 5 shows that the accuracy of SARIn is quite similar to the CFI retracker in LRM.

Different observation techniques have substantiated the stability of the surface elevation above Lake Vostok over time scales of typical satellite altimeter mission life times (Richter et al., 2008, 2014). This stability, together with the low precipitation and the continuous monitoring of relevant parameters at Vostok station, makes Lake Vostok an ideal area to examine apparent elevation variations in the altimetric time series. Spurious variations can be related to changes in surface backscatter and thus the backscattered power σ_0 of the altimetric signal (Wingham et al., 1998). Commonly, the relationship is determined as a regression coefficient and its influence is removed from the elevation time series (Wingham et al., 1998; Davis and Ferguson,

The Cryosphere Discuss., doi:10.5194/tc-2016-282, 2017
Manuscript under review for journal The Cryosphere
Published: 3 January 2017

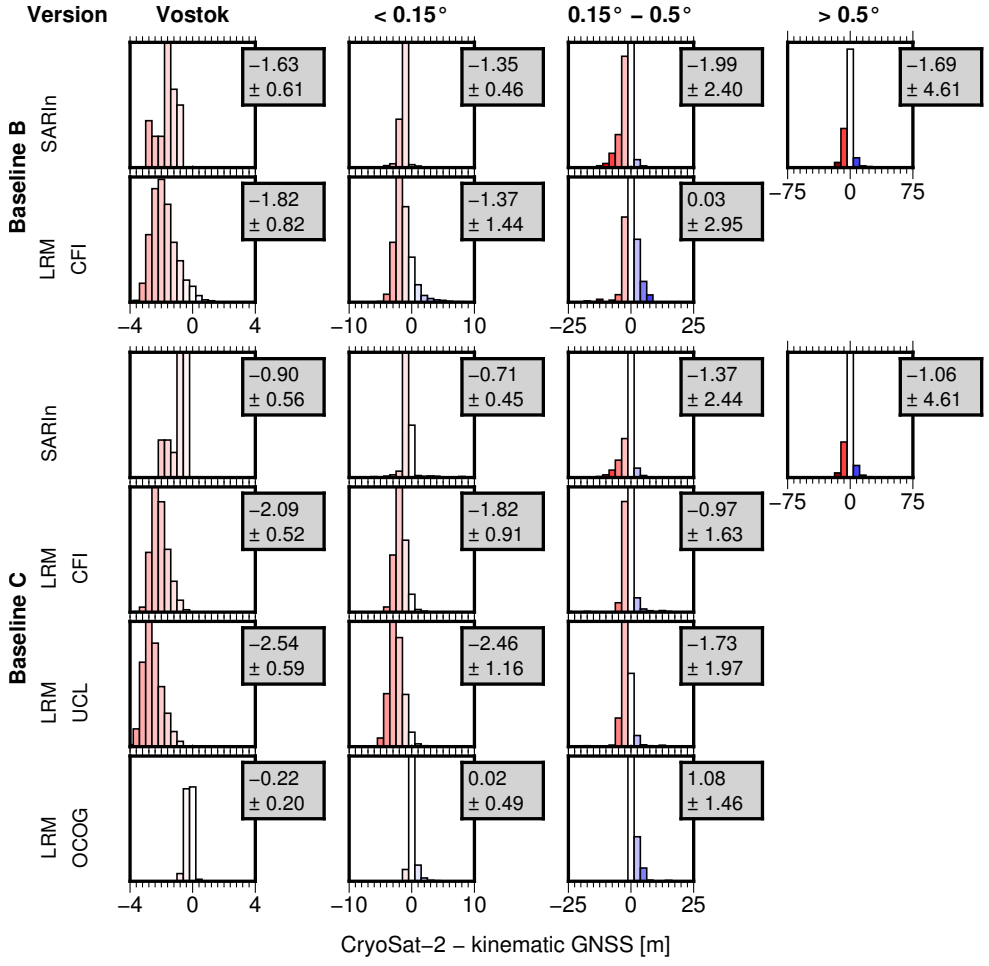

Figure 5. Histograms, means and standard deviations of crossover differences between different CryoSat-2 datasets and kinematic GNSS profiles for four zones of characteristic surface slope. The histogram ranges are the same as in Fig. 4 (Envisat) for comparability. The displayed crossover differences contain uncertainties in the kinematic GNSS profiles (4 - 9 cm) and possible elevation changes between the observation epochs of both techniques in addition to the uncertainty in the Cryosat data.

2004; Zwally et al., 2015). Figure 6 displays monthly averages of the crossover differences between the kinematic GNSS profiles and different CryoSat-2 LRM datasets. The Baseline B product (panel a) yields a high correlation as well as trends of opposite sign in the elevations and the backscatter values. A trend derived from this elevation dataset suggests a surface increase of 9.8 cm/yr which clearly contradicts all results from other studies. For the three retrackers of the Baseline C product (Fig. 6 b-d) none of the backscatter curves shows a significant trend any more. Nevertheless, the retracking methods based on functional fits (CFI in b, UCL in c) still exhibit a high correlation between Δh and σ_0. Here, the retracking point is defined by the fit of the functional model to the whole waveform. Hence, it is more affected by volume scattering. In contrast the OCOG retracker uses a 25% threshold of the OCOG amplitude and thus locates the retracking point much closer to the first radar return. The results in

The Cryosphere Discuss., doi:10.5194/tc-2016-282, 2017
Manuscript under review for journal The Cryosphere
Published: 3 January 2017

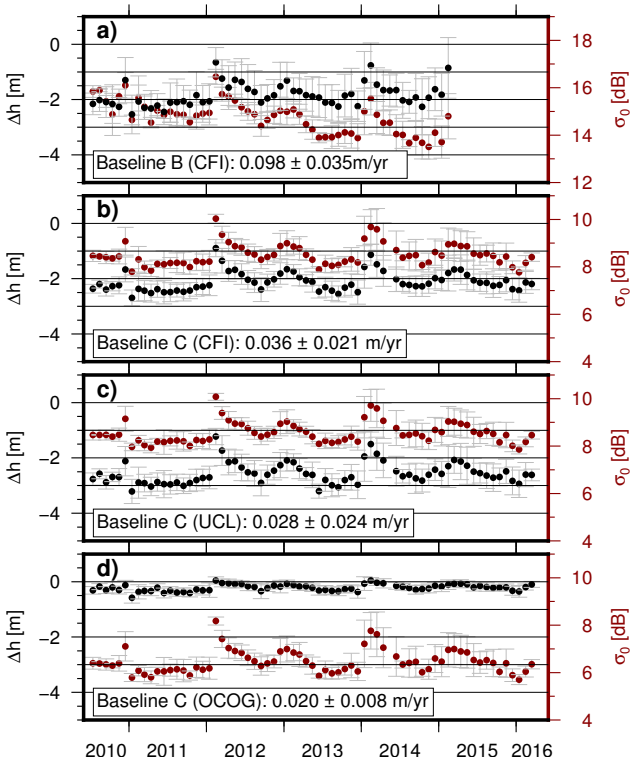

Figure 6. a-d) Monthly averages of crossover differences between different versions of CryoSat-2 data and kinematic GNSS profiles (black) and the corresponding backscatter σ_0 (red) within the hydrostatic equilibrium area of Lake Vostok. **a)** Baseline B dataset, **b-d)** Baseline C using the 3 different retrackers applied. The box at the bottom of each plot gives the overall elevation trend.

Fig. 6 indicate that threshold retrackers (panel d) produce the most precise elevations, especially in terms of repeatability. This confirms similar findings by Davis (1997). The seasonal variation of the signal almost vanishes. However, there is still a very small remaining amplitude, which correlates quite well with σ_0. This indicates that there might still be some remaining effects of the snowpack properties superimposed on the elevation time series. Once the large variations disappeared, some jumps of a few decimeters are revealed. Apparent height jumps in two winters correspond to abrupt backscatter increase at the same time. Lacroix et al. (2009) detected a similar jump in Envisat data and referred it to changes in snow pack properties due to strong wind. However, the meteorological records from Vostok station (wind, precipitation, temperature; not shown here) do not show any significant peak at the times of the jumps. Inconsistencies in the applied correction models of the ionosphere, troposphere and tides can be ruled out as origin of these jumps. None of the time series of these features show variations exceeding a few centimeters. Future studies including additional datasets will show whether these jumps are related to remaining processing issues or physical processes.

The Cryosphere Discuss., doi:10.5194/tc-2016-282, 2017
Manuscript under review for journal The Cryosphere
Published: 3 January 2017

Table 3. ICESat laser campaign biases (release 34) derived from a combined crossover adjustment of ICESat elevations and kinematic GNSS profiles over subglacial Lake Vostok (to be subtracted from the elevations for correction).

Laser campaign	Δh [cm]	Laser campaign	Δh [cm]
L1A	1.8 ± 0.8	L3F	3.7 ± 0.6
L2A	8.8 ± 0.8	L3G	7.1 ± 0.6
L2B	4.9 ± 0.7	L3H	4.6 ± 0.5
L2C	10.2 ± 0.7	L3I	4.6 ± 0.5
L3A	1.8 ± 0.8	L3J	7.1 ± 0.5
L3B	3.2 ± 0.7	L3K	8.2 ± 0.6
L3C	2.7 ± 0.6	L2D	10.4 ± 0.5
L3D	6.6 ± 0.6	L2E	13.2 ± 0.5
L3E	4.9 ± 0.6	L2F	10.5 ± 0.6

Table 4. Trends inferred from different sets of ICESat laser campaign biases weighted according to their standard deviation (if given). Results for Hofton (2013) differ from the originally given values as these authors applied unit weights. The trends in the second column have been calculated using only the laser campaigns Zwally et al. (2015) employed for their study.

set	$\dot{h}$ [cm/yr]	$\dot{h}_{L2A-L2D}$ [cm/yr]
This study	1.08 ± 0.35	0.57 ± 0.41
Richter (2014)	0.66 ± 0.45	0.33 ± 0.56
Hofton (2013) 86S	1.33 ± 0.36	1.11 ± 0.46
Hofton (2013) EAIS	1.72 ± 0.47	1.38 ± 0.53
Urban (2016)	0.01 ± 0.39	-0.44 ± 0.32
Zwally (2015)	-	-1.43 ± 0.44

3.3.3 ICESat

Prior to the validation of ICESat elevation data, we first determine the ICESat laser campaign biases as described in Sect. 3.2.2. The resulting biases are given in Table 3. The simultaneously derived surface-elevation change rate $\dot{h}$ from Eq. (4) amounts to 0.1 ± 0.1 cm/yr. This is a new, independent evidence for the stability of the surface elevation above Lake Vostok. It confirms our results in Sect. 2.5 and those of previous studies (Richter et al., 2008, 2014). It also justifies the assumption of a stable surface made by Ewert et al. (2012) and Richter et al. (2014) as a precondition for the campaign bias determination. It is, therefore, not surprising that our biases are very similar to the set presented by Richter et al. (2014) for R33 including the Gaussian-Centroid (G-C) correction. The major difference is an offset of about 5 cm. This arises from the fact that in this study, we perform an absolute calibration.

The Cryosphere Discuss., doi:10.5194/tc-2016-282, 2017
Manuscript under review for journal The Cryosphere
Published: 3 January 2017

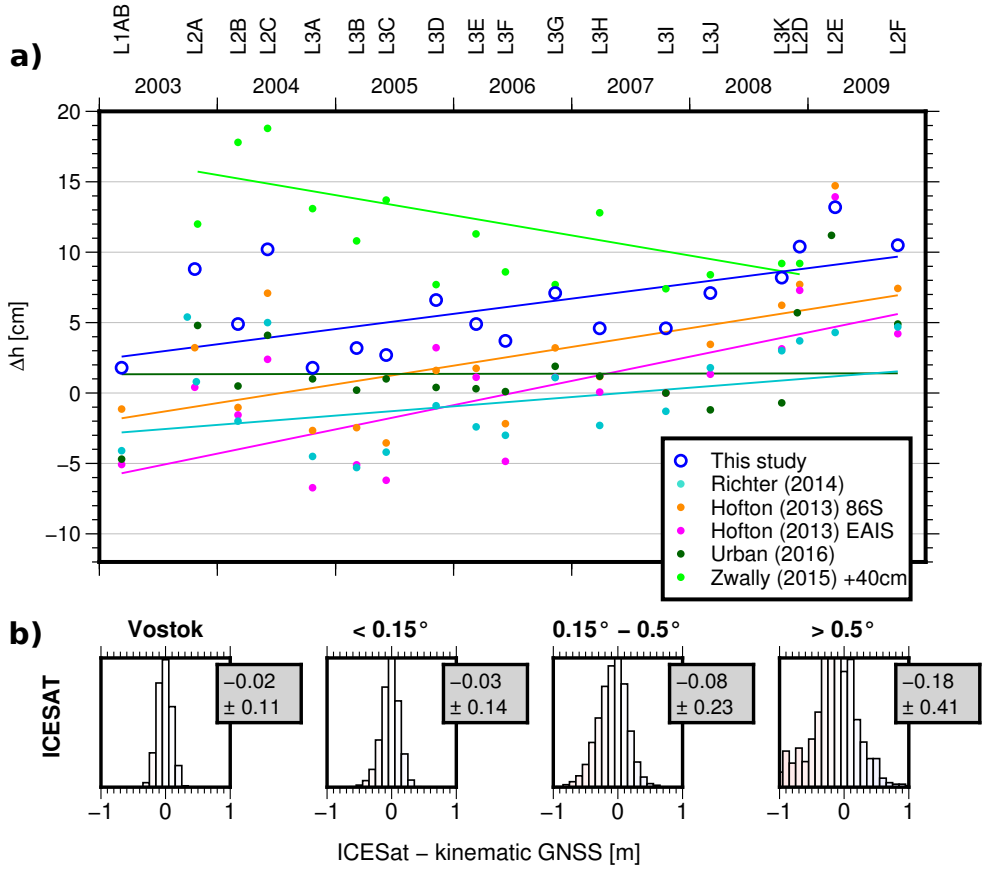

Figure 7. a) ICESat laser campaign biases (release 34) determined in the present study over Lake Vostok from inter-campaign crossovers and from crossovers with kinematic GNSS profiles (in dark blue) compared to other recently published bias sets and their trends. **b)** Histograms, means and standard deviations of crossover differences between ICESat and the kinematic GNSS profiles for four zones of characteristic surface slope. The range of the histograms is kept fixed to ±1 m. The displayed crossover differences contain uncertainties in the kinematic GNSS profiles (4 - 9 cm) and possible elevation changes between the observation epochs of both techniques in addition to the uncertainty in the ICESat data.

The chronological sequence of the laser campaign biases implies a trend which distorts any determination of surface-elevation rates if the biases are not applied. This trend over the entire ICESat operational period amounts to 1.08 ± 0.35 cm/yr. Table 4 and Fig. 7a compare the results of our new set of laser campaign biases with those of different recent publications. For consistency we limit this comparison to publications using either R33 data including G-C correction or R34. Hofton et al. (2013) used an internal crossover adjustment over the low precipitation zone of the East Antarctic Ice Sheet (EAIS) as well as absolute calibration using an ICEBridge lidar profile along the maximum latitudinal extent of the ICESat mission (86°S). To account for any possible elevation changes, the authors apply corrections for glacial isostatic adjustment (GIA) and firn densification. It is interesting to note that in principle both sets of their biases are very similar to our results but the artificial

The Cryosphere Discuss., doi:10.5194/tc-2016-282, 2017
Manuscript under review for journal The Cryosphere
Published: 3 January 2017

trends these biases imply are 0.2 to 0.6 cm/yr larger than our rates (Fig. 7a, column $\dot{h}$ in Table 4). This might be due to some unmodeled effects in the firn densification model and/or GIA correction of Hofton et al. (2013). Nevertheless, both of their sets of laser campaign biases (obtained in different regions of Antarctica and with different methods) agree with our results within their stated accuracies.

In contrast, the trends obtained by Urban (in Scambos and Shuman, 2016) and Zwally et al. (2015) from calibrations over the ocean differ significantly from the results of calibrations over Antarctica. Urban (in Scambos and Shuman, 2016), from a calibration over the global ocean, obtained significantly smaller biases. Zwally et al. (2015) calculated offsets from open water and thin ice in leads and polynyas in polar sea ice and used them to determine elevation changes over Antarctica. They obtain a $\dot{h}$ for Lake Vostok of 2.02 cm/yr. This contradicts the results of this study, but also those of two independent datasets in Richter et al. (2014), i.e. static GNSS observations and kinematic GNSS profiles using snow mobiles (compare Richter et al., 2016). It is interesting to note, however, that the trends implied by our laser campaign biases and those of Zwally et al. (2015) differ by 2.00 cm/yr. This explains the discrepancies of the elevation change rates obtained by Zwally et al. (2015) over Lake Vostok as a result of the applied set of laser campaign biases. The choice of these biases influences the derivation of elevation change rates from ICESat over the entire Antarctic ice sheet. Hence this explains the disparity between their ICESat-derived mass budget and the mass-balance estimates of many other studies (e.g. Shepherd et al., 2012; McMillan et al., 2014; Martín-Español et al., 2016), especially in East Antarctica.

After applying the laser campaign biases as corrections to the ICESat surface elevations we calculate the crossover differences with respect to the kinematic GNSS profiles. The results in Fig. 7b) show the very high accuracy of the ICESat data even in the coastal zone. The crossover differences in the less sloping regions indicate that both datasets have practically the same precision (compare Table 1). Close to the coast we observe a small increase in standard deviation (approx. 30 cm for slopes exceeding 0.5°). This might be an effect of the increased surface roughness which affects the interpolation of the elevation to the crossover point. Since we do not correct for any elevation changes in this comparison, these crossover differences also include any $\dot{h}$. The obtained small standard deviation, in turn, constrains the magnitude of possible elevation changes in these zones.

4 Validation of Digital Elevation Models

4.1 Data

Our kinematic GNSS profiles allow to validate not only altimetric surface elevations but also derived products such as gridded digital elevation models (DEMs). These products are used in a wide range of applications in polar sciences. In some cases, as the topographic correction in repeat track analysis (Moholdt et al., 2010) or the estimation of drainage basins (Zwally et al., 2012), only the accuracy of elevation differences between neighboring cells is important. Other applications, such as the derivation of ice thickness at the grounding line (Rignot et al., 2008) depend on the absolute accuracy.

We validate four DEMs of Antarctica derived from satellite altimetry. The 500 m resolution DEM from data of the ICESat mission by DiMarzio et al. (2007) (further called ICESat-DEM) was a milestone for many applications. Compared to previous,

The Cryosphere Discuss., doi:10.5194/tc-2016-282, 2017
Manuscript under review for journal The Cryosphere
Published: 3 January 2017

SRA-based DEMs, it provided a "greater latitudinal extent and fewer slope-related effects". Nevertheless, a weak spot was the coarse cross track spacing, especially for applications in coastal regions. The DEM by Bamber et al. (2009) (Bamber-DEM) overcame this problem by combining the high accuracy of ICESat with the high spatial resolution of ERS-1. The DEM produced by the Bedmap 2 project (Bedmap2-DEM) combined the Bamber-DEM with regional models in the margins, the ice shelves and the Antarctic Peninsula (Fretwell et al., 2013). To make the Bedmap2-DEM comparable, we converted the elevations from the GL04C geoid to WGS84 ellipsoid reference surface. Even though it should be identical to the Bamber-DEM for the major part of the region, we included this model to show the loss of accuracy by rounding towards integer meters as it has been done for Bedmap2.

In addition to these ICESat-dominated DEMs, Helm et al. (2014) compiled the first 3 years of the CryoSat-2 mission to a new DEM (CryoSat-DEM). With its improved design, the radar altimeter aboard CryoSat-2 is capable to provide very precise data in the margins. Furthermore, the high data density due to the orbit configuration allows to produce a very homogeneous dataset. There is almost no need to fill data gaps due to the very small across-track spacing.

4.2 Methods

By interpolating the DEM grid to the positions of the individual GNSS measurements using bicubic interpolation, we obtain an elevation difference for every single GNSS data location. Hence, the DEM validation relies on much more elevation differences than the validation of the altimetry profiles themselves, where the heights could only be compared at crossover locations.

To facilitate the comparison with the results from Sect. 3, we subdivide these elevation differences into the same zones as described in 3.2.1. In the validation of DEMs, special attention has to be paid to interpolation errors. The high resolution of 500 m of the ICESat-DEM seems reasonable when working with cells which contain measurements. However, no data exist within the almost 20 km gaps between the altimeter tracks. Thus, for a closer look into these interpolation errors, we examine the dependence of the elevation differences from the distance to the nearest track.

4.3 Results

The results of the validation (Fig. 8) of the ICESat-DEM shows that over Lake Vostok the accuracy is close to that of the original ICESat elevations. This indicates that in this case of exceptionally smooth topography the interpolation error is negligible. However, with increasing slope the standard deviation of this DEM grows fast due to the scarce across-track spacing of the altimetric profiles. In the Bamber-DEM, the inclusion of the additional ERS-1 data reduces this interpolation error between the ICESat tracks by 50% in terms of standard deviation. In the coastal zone, the gain in accuracy is minor as the precision of the radar altimetry data deteriorates.

The comparison of the Bedmap2-DEM with the Bamber-DEM reveals remarkable differences. Firstly, the rounding to integer elevations in Bedmap2 increases the standard deviation by several decimeters. Secondly, a constant offset of -1 m becomes evident in the Bedmap2 dataset. This seems to be an issue in the compilation procedure as the original Bamber-DEM shows a good agreement in terms of mean difference with our GNSS profiles in all regions. Finally, in the coastal zone the two models

The Cryosphere Discuss., doi:10.5194/tc-2016-282, 2017
Manuscript under review for journal The Cryosphere
Published: 3 January 2017

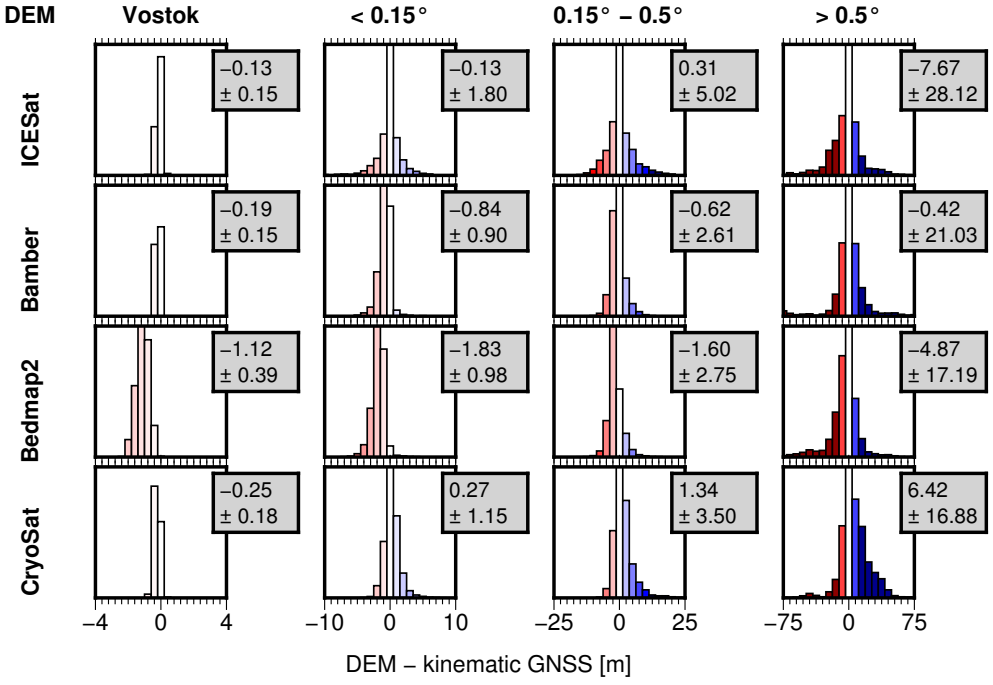

Figure 8. Histograms, means and standard deviations of differences between four different DEMs and kinematic GNSS profiles for four zones of characteristic surface slope.

behave differently. In Bedmap2 regional elevation models have been included here, but the sparse sampling of these areas by our profiles (see Fig. 3) does not allow a reliable evaluation.

The comparison of the CryoSat-DEM with the ICESat-based models proves that SRA with the advanced instrument design is able to provide accurate elevation information even in steep topography too. As for the CryoSat-2 altimetry data, a slope dependent offset is observed which presumably results from the systematic under-representation of local depressions.

In order to shed light on the relation of the DEM accuracy with the surface slope, the median absolute deviations (DEM vs. kinematic GNSS) are binned in 0.1 ° slope intervals (Fig. 9). The medians of the entire set of deviations (thick black lines) reveal a significant increase with the slope. Splitting the deviations into subsets according to the distance to the nearest ICESat track the impact of the interpolation error on a particular DEM becomes evident (panels a, b). It demonstrates the much greater dependence of the ICESat-DEM on the across-track distance compared to the Bamber-DEM. While the ICESat-DEM yields superior accuracy close to the tracks (i.e. distances < 1 km) due to its small grid interval (500 m), its median deviations exceed 10 m at large slopes (> 0.5°) and distances (> 6 km).

The dense spatial sampling of the CryoSat-2 altimetry data usually yields observed elevations for each cell of the CryoSat-DEM. According to the histograms obtained for the four zones, the slightly larger deviations of this DEM compared to the other models are mainly due to the slope dependent offset. The authors of this DEM provide an error map based on a validation

The Cryosphere Discuss., doi:10.5194/tc-2016-282, 2017
Manuscript under review for journal The Cryosphere
Published: 3 January 2017

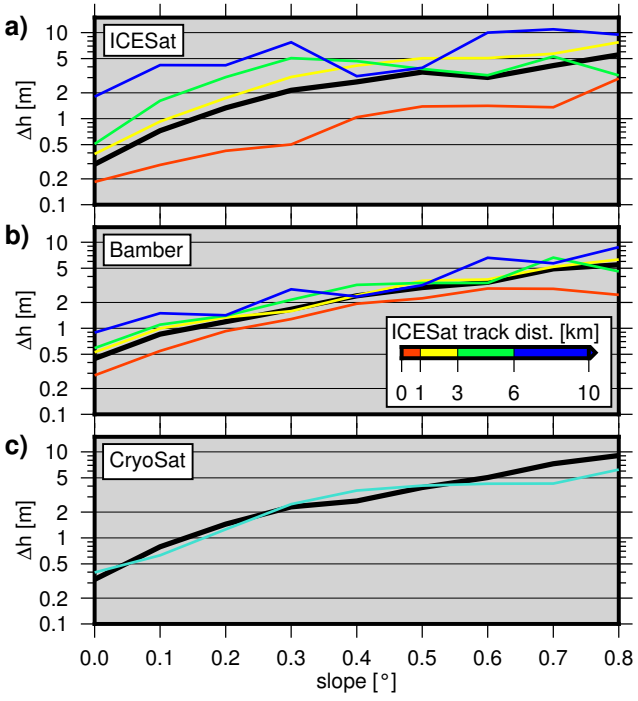

Figure 9. Median of absolute differences between various DEMs and the kinematic GNSS profiles binned by surface slope (thick black line). **a+b)** Additionally for DEMs based on ICESat - colored lines show the differences for several ranges of distances to the laser altimeter tracks (color coded). **c)** For the CryoSat-DEM the turquoise line shows the estimated error given by the uncertainty map which comes with the DEM.

with ICESat and airborne elevation data. These uncertainties are shown in Fig. 9c as a function of slope. Their good agreement with our results confirms them as realistic.

5 Conclusions

Between 2001 and 2015 we logged kinematic GNSS data along nine scientific traverses convoys and derived more than 30 000 km of surface-elevation profiles. We resolved the challenges of the GNSS processing, such as the very long baselines and peculiar vehicle dynamics in soft snow. Our elevation profiles have accuracies between 4 and 9 cm for a single data point. Over Lake Vostok crossover differences yield a mean elevation change rate of 0.3 ±0.5 cm/yr. This confirms the results of Richter et al. (2014) and qualifies this area as a calibration site for satellite altimetry.

A crossover analysis with three different Envisat elevation datasets reveals the impact of different processing strategies in satellite radar altimetry. Concerning the slope correction the relocation method is clearly superior to the direct method reducing elevation errors by about 66% in terms of standard deviation. Threshold retrackers (ICE1/OCOG) outperform functional fit retrackers by up to 50% in standard deviation. A similar analysis with CryoSat-2 LRM mode data confirms this finding. Hence,

The Cryosphere Discuss., doi:10.5194/tc-2016-282, 2017
Manuscript under review for journal The Cryosphere
Published: 3 January 2017

we recommend threshold retrackers for the determination of elevation time series because of its significant suppression of the snowpack related pseudo elevation variations.

ICESat elevation data and our kinematic GNSS profiles are comparable in their accuracy, even close to the coast. This comparison constrains also the magnitude of temporal elevation changes. A combined crossover adjustment above Lake Vostok yields a new set of ICESat laser campaign biases that no longer depends on an a-priori assumption of a stable surface elevation. The here obtained surface-elevation change rate of 0.1 ± 0.1 cm/yr proves nevertheless that this assumption is correct to a very high level of certainty. The correction of ICESat elevation data for the laser campaign biases is crucial for estimates of surface elevation change rates and the according mass balance. These biases are the main cause for the discrepancies between the ICESat-derived mass balances of Zwally et al. (2015) and those of other recent studies (see also Scambos and Shuman, 2016).

The validation of four digital elevation models demonstrates the reduction of interpolation errors achieved by Bamber et al. (2009) by complementing ICESat elevations with radar altimetry data. The advanced instrument design and high spatial resolution of CryoSat-2 permits now also radar altimetry to provide DEMs (Helm et al., 2014) of similar accuracy avoiding extensive interpolation.

Acknowledgements. This work is supported by the Deutsche Bundesstiftung Umwelt (DBU, German Federal Environmental Foundation). The fieldwork was partly funded by the German Research Foundation DFG (grants DI 473/20; DI 473/34; DI 473/38; SCHE1426/20-1) and the Russian Foundation for Basic Research (grant 10-05-91330-NNIO-a). We also thank the participants of the Russian Antarctic Expedition, especially the convoy teams, for their valuable support. We thank the NASA Goddard Space Flight Center, the European Space Agency and the National Snow and Ice Data Center for providing the altimetry data products.

The Cryosphere Discuss., doi:10.5194/tc-2016-282, 2017
Manuscript under review for journal The Cryosphere
Published: 3 January 2017

References

Arthern, R., Wingham, D., and Ridout, A.: Controls on ERS altimeter measurements over ice sheets: Footprint-scale topography, backscatter fluctuations, and the dependence of microwave penetration depth on satellite orientation, Journal of Geophysical Research – Atmospheres, 106, 33 471–33 484, 2001.

Bamber, J.: Ice Sheet Altimeter Processing Scheme, Int. J. Remote Sensing, 14, 925–938, 1994.

Bamber, J., Gomez-Dans, J., and Griggs, J.: A new 1 km digital elevation model of the Antarctic derived from combined satellite radar and laser data – Part 1: Data and methods, The Cryosphere, 3, 101–111, doi:10.5194/tc-3-101-2009, 2009.

Bouffard, J.: Level 2 product evolutions and quality improvements in Baseline C, Tech. rep., 2015.

Brenner, A., Bindschadler, R., Zwally, H., and Thomas, R.: Slope-induced errors in radar altimetry over continental ice sheets, J. Geophys. Res., 88, 1617–1623, doi:10.1029/JC088iC03p01617, 1983.

Brenner, A., DiMarzio, J., and Zwally, H.: Precision and Accuracy of Satellite Radar and Laser Altimeter Data Over the Continental Ice Sheets, IEEE Trans. Geosci. Remote Sens., 45, 321–331, doi:10.1109/TGRS.2006.887172, 2007.

Dach, R., Lutz, S., Walser, P., and Fridez, P., eds.: Bernese GNSS Software Version 5.2, Astronomical Institute, University of Bern, Bern Open Publishing, Bern, doi:10.7892/boris.72297, 2015.

Davis, C.: A robust threshold retracking algorithm for measuring ice-sheet surface elevation change from satellite radar altimeters, Geoscience and Remote Sensing, IEEE Transactions on, 35, 974–979, doi:10.1109/36.602540, 1997.

Davis, C. and Ferguson, A.: Elevation change of the Antarctic ice sheet, 1995-2000, from ERS-2 satellite radar altimetry, IEEE Trans. Geosci. Remote Sens., 42, 2437–2445, doi:10.1109/TGRS.2004.836789, 2004.

DiMarzio, J., Brenner, A., Schutz, B., Shuman, C., and Zwally, H.: GLAS/ICESat 500 m Laser Altimetry Digital Elevation Model of Antarctica, Version 1, National Snow and Ice Data Center, Boulder, Colorado USA, doi:http://dx.doi.org/10.5067/K2IMI0L24BRJ, 2007.

Ekaykin, A., Vladimirova, D., Lipenkov, V., and Masson-Delmotte, V.: Climatic variability in Princess Elizabeth Land (East Antarctica) over the last 350 years, Climate of the Past Discussions, 2016, 1–21, doi:10.5194/cp-2016-76, 2016.

ESA: ENVISAT RA2/MWR Product Handbook, 2007.

Ewert, H., Popov, S., Richter, A., Schwabe, J., Scheinert, M., and Dietrich, R.: Precise analysis of ICESat altimetry data and assessment of the hydrostatic equilibrium for subglacial Lake Vostok, East Antarctica, Geophys. J. Int., 191, 557–568, doi:10.1111/j.1365-246X.2012.05649.x, 2012.

Flament, T. and Rémy, F.: Antarctica volume change from 10 years of Envisat altimetry, in: Geoscience and Remote Sensing Symposium (IGARSS), 2012 IEEE International, pp. 1848–1851, doi:10.1109/IGARSS.2012.6351149, 2012.

Fretwell, P., Pritchard, H., Vaughan, D., Bamber, J., Barrand, N., Bell, R., Bianchi, C., Bingham, R., Blankenship, D., Casassa, G., Catania, G., Callens, D., Conway, H., Cook, A., Corr, H., Damaske, D., Damm, V., Ferraccioli, F., Forsberg, R., Fujita, S., Gim, Y., Gogineni, P., Griggs, J., Hindmarsh, R., Holmlund, P., Holt, J., Jacobel, R., Jenkins, A., Jokat, W., Jordan, T., King, E., Kohler, J., Krabill, W., Riger-Kusk, M., Langley, K., Leitchenkov, G., Leuschen, C., Luyendyk, B., Matsuoka, K., Mouginot, J., Nitsche, F., Nogi, Y., Nost, O., Popov, S., Rignot, E., Rippin, D., Rivera, A., Roberts, J., Ross, N., Siegert, M., Smith, A., Steinhage, D., Studinger, M., Sun, B., Tinto, B., Welch, B., Wilson, D., Young, D., Xiangbin, C., and Zirizzotti, A.: Bedmap2: improved ice bed, surface and thickness datasets for Antarctica, The Cryosphere, 7, 375–393, doi:10.5194/tc-7-375-2013, 2013.

Fricker, H., Borsa, A., Minster, B., Carabajal, C., Quinn, K., and Bills, B.: Assessment of ICESat performance at the salar de Uyuni, Bolivia, Geophys. Res. Lett., 32, L21S06, doi:10.1029/2005GL023423, 2005.

Fritsche, M., Sośnica, K., Rodríguez-Solano, C., Steigenberger, P., Wang, K., Dietrich, R., Dach, R., Hugentobler, U., and Rothacher, M.: Homogeneous reprocessing of GPS, GLONASS and SLR observations, J. Geod., 88, 625–642, doi:10.1007/s00190-014-0710-3, 2014.

Groh, A., Ewert, H., Rosenau, R., Fagiolini, E., Gruber, C., Floricioiu, D., Abdel Jaber, W., Linow, S., Flechtner, F., Eineder, M., Dierking, W., and Dietrich, R.: Mass, volume and velocity of the Antarctic Ice Sheet: present-day changes and error effects, Surv. Geophys., 35, 1481–1505, doi:10.1007/s10712-014-9286-y, 2014.

Gunter, B., Urban, T., Riva, R., Helsen, M., Harpold, R., Poole, S., Nagel, P., Schutz, B., and Tapley, B.: A comparison of coincident GRACE and ICESat data over Antarctica, J. Geod., 83, 1051–1060, doi:10.1007/s00190-009-0323-4, 2009.

Gunter, B., Didova, O., Riva, R., Ligtenberg, S., Lenaerts, J., King, M., van den Broeke, M., and Urban, T.: Empirical estimation of present-day Antarctic glacial isostatic adjustment and ice mass change, The Cryosphere, 8, 743–760, doi:10.5194/tc-8-743-2014, 2014.

Helm, V., Humbert, A., and Miller, H.: Elevation and elevation change of Greenland and Antarctica derived from CryoSat-2, The Cryosphere, 8, 1539–1559, doi:10.5194/tc-8-1539-2014, 2014.

Hofton, M., Luthcke, S., and Blair, J.: Estimation of ICESat intercampaign elevation biases from comparison of lidar data in East Antarctica: Estimating ICESat elevation biases, Geophys. Res. Lett., 40, 5698–5703, doi:10.1002/2013GL057652, 2013.

Kohler, J., Neumann, T., Robbins, J., Tronstad, S., and Melland, G.: ICESat Elevations in Antarctica Along the 2007–09 Norway-USA Traverse: Validation With Ground-Based GPS, IEEE Trans. Geosci. Remote Sens., 51, 1578–1587, doi:10.1109/TGRS.2012.2207963, 2013.

Lacroix, P., Legrésy, B., Rémy, F., Blarel, F., Picard, G., and Brucker, L.: Rapid change of snow surface properties at Vostok, East Antarctica, revealed by altimetry and radiometry, Remote Sens. Environ., 113, 2633–2641, doi:10.1016/j.rse.2009.07.019, 2009.

Legrésy, B., Papa, F., Rémy, F., Vinay, G., van den Bosch, M., and Zanife, O.-Z.: ENVISAT radar altimeter measurements over continental surfaces and ice caps using the ICE-2 retracking algorithm, Remote Sens. Environ., 85, 150–163, doi:10.1016/j.rse.2004.11.018, 2005.

Luthcke, S., Rowlands, D., Williams, T., and Sirota, M.: Reduction of ICESat systematic geolocation errors and the impact on ice sheet elevation change detection, Geophys. Res. Lett., 32, L21S05, doi:10.1029/2005GL023689, 2005.

Martín-Español, A., Zammit-Mangion, A., Clarke, P., Flament, T., Helm, V., King, M., Luthcke, S., Petrie, E., Rémy, F., Schön, N., Wouters, B., and Bamber, J.: Spatial and temporal Antarctic Ice Sheet mass trends, glacio-isostatic adjustment and surface processes from a joint inversion of satellite altimeter, gravity and GPS data, J. Geophys. Res. Earth Surf., 121, 182–200, doi:10.1002/2015JF003550, 2016.

Masolov, V., Lukin, V., Sheremetiev, A., and Popov, S.: Geophysical Investigations of the Subglacial Lake Vostok in Eastern Antarctica, Doklady Earth Sciences, 379A, 734–738, 2001.

McCarthy, D. and Petit, G., eds.: IERS Conventions (2003), vol. 32 of *IERS Technical Note*, Verlag des Bundesamts für Kartographie und Geodäsie, Frankfurt am Main, 2004.

McMillan, M., Shepherd, A., Sundal, A., Briggs, K., Muir, A., Ridout, A., Hogg, A., and Wingham, D.: Increased ice losses from Antarctica detected by CryoSat-2, Geophys. Res. Lett., 41, 3899–3905, doi:10.1002/2014GL060111, 2014.

Moholdt, G., Nuth, C., Hagen, J., and Kohler, J.: Recent elevation changes of Svalbard glaciers derived from ICESat laser altimetry, Remote Sens. Environ., 114, 2756–2767, doi:10.1016/j.rse.2010.06.008, 2010.

Petit, G. and Luzum, B., eds.: IERS Conventions (2010), vol. 36 of *IERS Technical Note*, Verlag des Bundesamts für Kartographie und Geodäsie, Frankfurt am Main, Germany, 2010.

Popov, S.: Recent Russian remote sensing investigations in Antarctica within the framework of scientific traverses, Advances in Polar Sciences, 26, 113–121, 2015.

Popov, S. and Chernoglazov, Y.: Podlednikovoe ozero Vostok, Vostochnaya Antarktida: beregovaya liniya i okruzhayushchie vodoemy [Vostok Subglacial Lake, East Antarctica: lake shoreline and subglacial water caves], Ice and Snow, N1(113), 12–24, 2011.

Richter, A., Popov, S., Dietrich, R., Lukin, V., Fritsche, M., Lipenkov, V., Matveev, A., Wendt, J., Yuskevich, A., and Masolov, V.: Observational evidence on the stability of the hydro-glaciological regime of subglacial Lake Vostok, Geophys. Res. Lett., 35, L11 502, doi:10.1029/2008GL033397, 2008.

Richter, A., Fedorov, D., Fritsche, M., Popov, S., Lipenkov, V., Ekaykin, A., Lukin, V., Matveev, A., Grebnev, V., Rosenau, R., and Dietrich, R.: Ice flow velocities over Vostok Subglacial Lake, East Antarctica, determined by 10 years of GNSS observations, J. Glac., 59, 315–326, doi:10.3189/2013JoG12J056, 2013.

Richter, A., Popov, S., Fritsche, M., Lukin, V., Matveev, A., Ekaykin, A., Lipenkov, V., Fedorov, D., Eberlein, L., Schröder, L., Ewert, H., Horwath, M., and Dietrich, R.: Height changes over subglacial Lake Vostok, East Antarctica: Insights from GNSS observations, J. Geophys. Res. Earth Surf., 119, 2460–2480, doi:10.1002/2014JF003228, 2014.

Richter, A., Horwath, M., and Dietrich, R.: Comment on Zwally and others (2015)-Mass gains of the Antarctic ice sheet exceed losses, J. Glac., pp. 1–3, doi:10.1017/jog.2016.60, 2016.

Ridley, J. and Partington, K.: A model of satellite radar altimeter return from ice sheets, Int. J. Remote Sensing, 9, 601–624, doi:10.1080/01431168808954881, 1988.

Rignot, E., Bamber, J., van den Broeke, M., Davis, C., Li, Y., van de Berg, W., and van Meijgaard, E.: Recent Antarctic ice mass loss from radar interferometry and regional climate modelling, Nature Geosci., 1, 106–110, doi:10.1038/ngeo102, 2008.

Roemer, S., Legrésy, B., Horwath, M., and Dietrich, R.: Refined analysis of radar altimetry data applied to the region of the subglacial Lake Vostok / Antarctica, Remote Sens. Environ., 106, 269–284, doi:10.1016/j.rse.2006.02.026, 2007.

Scagliola, M. and Fornari, M.: Main evolutions and expected quality improvements in BaselineC Level1b products, Tech. rep., 2015.

Scambos, T. and Shuman, C.: Comment on 'Mass gains of the Antarctic ice sheet exceed losses' by H. J. Zwally and others, J. Glac., pp. 1–5, doi:10.1017/jog.2016.59, 2016.

Schutz, B., Zwally, H., Shuman, C., Hancock, D., and DiMarzio, J.: Overview of the ICESat Mission, Geophys. Res. Lett., 32, L21S01, doi:10.1029/2005GL024009, 2005.

Shepherd, A., Ivins, E., A, G., Barletta, V., Bentley, M., Bettadpur, S., Briggs, K., Bromwich, D., Forsberg, R., Galin, N., Horwath, M., Jacobs, S., Joughin, I., King, M., Lenaerts, J., Li, J., Ligtenberg, S., Luckman, A., Luthcke, S., McMillan, M., Meister, R., Milne, G., Mouginot, J., Muir, A., Nicolas, J., Paden, J., Payne, A., Pritchard, H., Rignot, E., Rott, H., Sorensen, L., Scambos, T., Scheuchl, B., Schrama, E., Smith, B., Sundal, A., van Angelen, J., van de Berg, W., van den Broeke, M., Vaughan, D., Velicogna, I., Wahr, J., Whitehouse, P., Wingham, D., Yi, D., Young, D., and Zwally, H.: A Reconciled Estimate of Ice-Sheet Mass Balance, Science, 338, 1183–1189, doi:10.1126/science.1228102, 2012.

Siegfried, M., Hawley, R., and Burkhart, J.: High-Resolution Ground-Based GPS Measurements Show Intercampaign Bias in ICESat Elevation Data Near Summit, Greenland, Geoscience and Remote Sensing, IEEE Transactions on, 49, 3393–3400, doi:10.1109/TGRS.2011.2127483, 2011.

Wanninger, L.: Interpolation von GPS-Beobachtungen, Allg. Vermnachr., 107, 360–363, heft 10/2000, 2000.

Wingham, D., Rapley, C., and Griffiths, H.: New techniques in satellite altimeter tracking systems, in: ESA Proceedings of the 1986 International Geoscience and Remote Sensing Symposium(IGARSS'86) on Remote Sensing: Today's Solutions for Tomorrow's Information Needs,, vol. 3, pp. 1339–1344, 1986.

Wingham, D., Ridout, A., Scharroo, R., Arthern, R., and Shum, C.: Antarctic Elevation Change from 1992 to 1996, Science, 282, 1998.

The Cryosphere Discuss., doi:10.5194/tc-2016-282, 2017
Manuscript under review for journal The Cryosphere
Published: 3 January 2017

Wingham, D., Francis, C., Baker, S., Bouzinac, C., Brockley, D., Cullen, R., Chateau-Thierry, P. d., Laxon, S., Mallow, U., Mavrocordatos, C., Phalippou, L., Ratier, G., Rey, L., Rostan, F., Viau, P., and Wallis, D.: CryoSat: A mission to determine the fluctuations in Earth's land and marine ice fields, Adv. Space Res., 37, 841–871, doi:10.1016/j.asr.2005.07.027, 2006a.

Wingham, D., Shepherd, A., Muir, A., and Marshall, G.: Mass balance of the Antarctic ice sheet, Phil. Trans. R. Soc. Lond. A, 364, 1627–1635, doi:10.1098/rsta.2006.1792, 2006b.

Zwally, H., Giovinetto, M., Beckley, M., and Saba, J.: Antarctic and Greenland Drainage Systems, 2012.

Zwally, H., Li, J., Robbins, J., Saba, J., Yi, D., and Brenner, A.: Mass gains of the Antarctic ice sheet exceed losses, J. Glac., 61, 1019–1936, 2015.